NIH Public Access
Author Manuscript
Mater Sci Eng C Mater Biol Appl. Author manuscript; available in PMC 2012 July 20.

Published in final edited form as:
Mater Sci Eng C Mater Biol Appl. 2011 July 20; 31(5): 945–949. doi:10.1016/j.msec.2011.02.016.

Quasi-static Torsional Deformation Behavior of Porous Ti6Al4V alloy

Vamsi Krishna Balla[2], **Shantel Martinez**[1], **Ben Tunberg Rogoza**[1], **Chase Livingston**[1], **Deepak Venkateswaran**[1], **Susmita Bose**[2], and **Amit Bandyopadhyay**[2,*]

[1]School of Chemical Engineering and Bioengineering, Washington State University, Pullman, WA 99164, USA

[2]W. M. Keck Biomedical Materials Research Laboratory, School of Mechanical and Materials Engineering, Washington State University, Pullman, WA 99164, USA

Abstract

Laser processed Ti6Al4V alloy samples with total porosities of 0%, 10% and 20% have been subjected to torsional loading to determine mechanical properties and to understand the deformation behavior. The torsional yield strength and modulus of porous Ti alloy samples was found to be in the range of 185-332 MPa and 5.7-11 GPa, respectively. With an increase in the porosity both the strength and the modulus decreased, and at 20% porosity the torsional modulus of Ti6Al4V alloy was found to be very close to that of human cortical bone. Further, the experiments revealed clear strain hardening and ductile deformation in all the samples, which suggests that the inherent brittleness associated solid-state sintered porous materials can be completely eliminated via laser processing for load bearing metal implant applications.

Keywords

laser deposition; torsion test; porous material; titanium alloy; deformation

1. Introduction

Metallic biomaterials currently in use for load-bearing orthopedic applications are bioinert and lack sufficient osseointegration for implant longevity [1]. One consideration to improve the healing process is focused on the use of porous metals, which can support tissue adhesion, growth and osseointegration. Moreover, porous metals can eliminate problems associated with stress shielding by tailoring their elastic modulus to match that of natural bone [1-5]. Many researchers have focused on obtaining desired mechanical properties in porous metallic biomaterials by controlling porosity characteristics via variety of fabrication techniques [3, 6-9]. While these studies provide good understanding of deformation and mechanical behavior of porous metals under tensile and compressive loads, the results may not be directly applicable to the deformation behavior and mechanical properties of porous metals under other modes of loading such as bending and torsion. Despite their physiological and mechanical relevance, the possible influence of highly complex *in vivo*

© 2011 Elsevier B.V. All rights reserved.

* Corresponding-Author: Prof. Amit Bandyopadhyay, Tel: 509-335-4862; amitband@wsu.edu.

Publisher's Disclaimer: This is a PDF file of an unedited manuscript that has been accepted for publication. As a service to our customers we are providing this early version of the manuscript. The manuscript will undergo copyediting, typesetting, and review of the resulting proof before it is published in its final citable form. Please note that during the production process errors may be discovered which could affect the content, and all legal disclaimers that apply to the journal pertain.

NIH-PA Author Manuscript
NIH-PA Author Manuscript
NIH-PA Author Manuscript

NIH-PA Author Manuscript

NIH-PA Author Manuscript

NIH-PA Author Manuscript

loading conditions on the deformation behavior of porous metallic biomaterials has rarely been considered. Although some studies report quasi-static and dynamic deformation of dense Ti6Al4V alloy under torsional loading [10-12], in particular, work on torsional behavior of porous Ti6Al4V alloy with clinical relevance is rather scarce. Therefore, in the present work, we have evaluated the influence of porosity (0 to 20%) on the mechanical properties and deformation behavior of laser processed Ti6Al4V alloy under torsional loading. This article also highlights the importance of laser processing, where the porosity forms as a result of localized melting and subsequent solidification, in contrast to solid-state sintering in the powder metallurgical route – leading to brittleness and loss of physical properties [13-15].

2. Materials and Methods

Ti6Al4V alloy powder (Advanced Speciality Metals Inc., NH, USA) with a size range of 50–150μm was used to prepare porous samples using Laser Engineering Net Shaping - LENS™750 system (Optomec Inc., Albuquerque, NM, USA). Detailed description and capabilities of LENS™ process can be found elsewhere [3, 7-9]. Our earlier work [5] showed that the modulus of laser processed Ti6Al4V alloy samples with total porosity > 25% was less than 10 GPa and are not suitable for direct load bearing implant applications though they may be used as coatings or scaffolds. Since the focus in this paper is to understand the influence of porosity on torsional deformation under load bearing environment, porous Ti6Al4V alloy samples with 0%, 10% and 20% total porosity were fabricated using (i) 350 W laser power, 17 mm s^{-1} scan speed, 12 g min^{-1} powder feed rate, (ii) 300 W, 15 mm s^{-1}, 20 g min^{-1}, and (iii) 250 W, 20 mm s^{-1}, 23 g min^{-1}, respectively.

Samples for torsion tests with 12 mm square ends and ϕ 10 mm in the gauge length (35 mm) were prepared directly from a 3-dimensional computer aided model. As-fabricated samples were tested at room temperature for their torsional properties and deformation behavior using a 220 Nm torsion testing machine (Instron-55 MT, Norwood, MA). All samples were tested until failure or 40% drop in torque at a torsional speed of 45° min^{-1}. From the torque - degrees of rotation data recorded during the test, torsional yield strength, modulus, maximum shear stress and strain were calculated and average of three tests (for each porosity) is reported along with standard deviation. Quasi-static compression tests for mechanical property evaluation were also carried out using a servo-hydraulic MTS (axial/torsion materials test system) machine with 250kN capacity at a strain rate of $10^{-3}s^{-1}$. Young's modulus and 0.2% proof strength were determined from the stress–strain plots derived from load–displacement data recorded during compression testing. A regression analysis was performed on all test data and $p < 0.05$ was considered statistically significant. The fractured surfaces of torsion samples were studied using field-emission scanning electron microscopy (FEI – Quanta 200F) to understand the influence of porosity on the deformation and failure mechanisms. Cross-sectional microstructures of the samples were also examined using FE-SEM. Vickers microhardness measurements were also made on the as-fabricated porous Ti6Al4V alloy samples using a 500g load for 15 s, and the average value of 10 measurements was reported.

Finally, to ensure that laser processing does not have any toxic influence on Ti6Al4V alloy samples, all the samples were evaluated for their *in vitro* cytotoxicity using MTT assay. All samples were sterilized by autoclaving at 121°C for 20 min. In this study, the cells used were an immortalized, cloned osteoblastic precursor cell line 1 (OPC1), which was derived from human fetal bone tissue [16] OPC1 cells were seeded onto the samples placed in 24-well plates. Initial cell density was 2.0×10^4cells $well^{-1}$. A 1 ml aliquot of McCoy's 5A medium (enriched with 5% fetal bovine serum, 5% bovine calf serum and supplemented with 4μg ml^{-1} of fungizone) was added to each well. Cultures were maintained at 37°C

NIH-PA Author Manuscript

NIH-PA Author Manuscript

NIH-PA Author Manuscript

under an atmosphere of 5% CO_2. Medium was changed every 2–3 days for the duration of the experiment. Samples for MTT assay were removed from culture at 3, 7 and 11 days of incubation. The MTT (Sigma, St. Louis, MO) solution of 5mg ml^{-1} was prepared by dissolving 3-(4,5-dimethylthiazole-2-yl)-2,5-diphenyl tetrazolium bromide (MTT) in phosphate-buffered saline and filter sterilizing it. The MTT was diluted (50μl into 450μl) in serum-free, phenol red-free Dulbecco's minimum essential medium. Then 500 μl of diluted MTT solution was added to each sample in 24-well plates. After 2h of incubation, 500μl of solubilization solution made up of 10% Triton X-100, 0.1N HCl and isopropanol was added to dissolve the formazan crystals. Then 100μl of the resulting supernatant was transferred into a 96-well plate and read by a plate reader at 570nm. Data are presented as mean ±standard deviation. Statistical analysis was performed using Student's t-test and $p < 0.05$ was considered statistically significant.

3. Results and Discussion

3.1 Microstructures

Figure 1 shows the microstructural features of laser processed Ti6Al4V alloy samples with different porosities. Fully dense samples showed characteristic Widmanstätten microstructure and porous Ti alloy samples exhibited more or less equiaxed α+β microstructures. In the Widmanstätten microstructure, the width of α platelets varied between 2 and 11 μm (average: 4.6 ± 2 μm) and the length was in the range of 10 and 100 μm (average: 38 ± 19 μm). The average α phase size was found to be 9.3 ± 4.5 μm and 13.4 ± 5.5 μm in the porous Ti alloy samples with 10% and 20% porosity, respectively. The observed variations in microstructural features of laser processed Ti alloy samples with different porosities is attributed to the variations in peak temperatures and cooling rates depending on the extent of powder melting as a result of laser parameters [9]. The Widmanstätten microstructure of fully dense Ti6Al4V alloy sample resulted in relatively high hardness of 284 ± 6 HV than porous Ti alloy samples with equiaxed α+β microstructures, 251 ± 11 HV and 259 ± 10 HV for 10% and 20% porous samples, respectively. Similar higher hardness of Widmanstätten microstructures than that of equiaxed microstructures has been reported in wrought Ti6Al4V alloy samples [11] and electron beam rapid manufactured Ti6Al4V alloy [17].

3.2 Mechanical Properties

Figure 2 shows typical shear stress – shear strain curves of laser processed Ti6Al4V alloy samples with different porosity. The torsional yield strength, failure stress and failure strain of present porous Ti6Al4V alloy are significantly higher than that of human cortical bone [18]. However, the torsional modulus of Ti6Al4V alloy with 20% porosity is very close to the modulus of cortical bone. Ti alloy samples with different porosities showed more or less similar level of strain hardening after yielding, and the stress increased continuously with strain until final fracture/failure. The torsional properties determined from these curves are summarized in Table 1, where compression properties are also included for comparison. The experimental results show that the torsional properties (maximum shear stress and shear strain) of present fully dense laser processed Ti6Al4V alloy samples with Widmanstätten microstructure (α platelets = 4.6 ± 2 μm) closely match with that of wrought Ti6Al4V alloy [11] with identical microstructure (α platelets = 5 to 6 μm). These results demonstrate that LENS™ has the ability to produce Ti alloy parts with torsional mechanical properties comparable to that of equivalent wrought alloy products.

Our experimental results clearly show that porosity can significantly decrease the mechanical properties of laser processed Ti6Al4V alloy both in compression and in torsional loading. As expected, torsional and compressive mechanical properties of laser processed

NIH-PA Author Manuscript

NIH-PA Author Manuscript

NIH-PA Author Manuscript

fully dense (0% porosity) Ti6Al4V alloy samples are higher than those of samples with 10 and 20% porosity. Initial addition of 10% porosity resulted in ~ 43%, ~ 48% and ~ 30% decrease in torsional yield strength, maximum shear stress and shear strain, respectively. Further increase in the porosity from 10% to 20% resulted in marginal decrease in torsional properties of laser processed Ti alloy samples. However, the maximum shear strain and shear strain at maximum shear stress dropped significantly (~ 58%) with an increase in the porosity from 10% to 20%. From the present results it is clear that the porous metal develops a shearing failure in torsion at a shear strain considerably lower than that required to develop a shear band within the fully dense material. This is consistent with our intuitive expectations that the pores should provide a destabilizing influence on the shearing deformation [19, 20]. Therefore, the porous Ti6Al4V alloy samples failed at lower shear stresses and strains compared to fully dense samples.

Comparison of yield strength of porous Ti alloy samples showed an approximately 8% decrease during compression loading and 43% decrease during torsional loading due to the presence of 10% porosity. This discrepancy can be explained based on the differences in deformation behavior of porous metals depending on the type of loading. Under uniaxial compressive loading, the porous Ti alloy samples densify as a result of pore closure and the stress increases rapidly. However, during torsional loading densification do not occur and the stress increases due to pure metal matrix strain hardening. Further, the presence of porosity can act as stress raiser during torsional loading leading to crack initiation at relatively low stresses. Because of these differences in deformation mechanisms, the decrease in mechanical properties of laser processed porous Ti6Al4V alloy samples, due to porosity, is more severe under torsional loading than observed during uniaxial compressive loading. However, the presence of stain hardening in laser processed porous Ti6Al4V alloy samples suggests that these samples deformed in ductile manner and thus the bonding between the particles is very strong. This is because the particle bonding during LENS™ processing is a direct result of localized melting and subsequent solidification [7, 9], in contrast to solid state sintering in powder metallurgical route. Therefore, the inherent brittleness associated with solid state sintered metal powders is completely eliminated in laser processed samples.

During quasi-static torsional deformation the Ti6Al4V alloy fail by fine void nucleation, at α/β interfaces or grain boundary α phase, and their coalescence [11]. Therefore, the alloy with fine Widmanstätten microstructures (large number/area of the interfaces) should exhibit least resistance to void nucleation and hence the quasi-static torsional properties than coarse equiaxed microstructures. In line with the above discussion, torsional properties of wrought Ti6Al4V alloy with Widmanstätten microstructures have been reported to be lower than that of equiaxed microstructures [11]. Although microstructurally more resistant to torsional deformation, present porous samples with equiaxed microstructures failed at relatively lower stresses/strains than fully dense samples with Widmanstätten microstructure. This is because the existing porosity in the present porous Ti6Al4V alloy samples can accelerate the void nucleation and coalescence due to strain localization near the pores and local destabilization of shear deformation, and thus decreasing the failure stress/strain. This can be clearly seen from significant drop (~ 58%) in the maximum shear strain and shear strain at maximum shear stress with an increase in the porosity from 10% to 20%. However, the benefit of equiaxed microstructure can be seen from comparable strain hardening behavior of porous samples to that of fully dense samples.

SEM fractographs of quasi-statically fractured torsional specimens are shown in Figure 3. All the samples show a typical ductile fracture mode composed of dimples. The dimple sizes of each sample closely match with the size of α platelets or phase in respective microstructures. Thus, dimple size increases in the order of Widmanstätten and equiaxed

NIH-PA Author Manuscript

NIH-PA Author Manuscript

NIH-PA Author Manuscript

microstructures because the initiation sites and number of voids vary with the microstructures. Within the porous samples notable difference in fracture surface is apparent, as shown in Figures 3b and 3c. The fracture morphology was coarse in 20% porous samples compared to 10% porous samples, which can be correlated to the grain/α phase size/morphology of these samples, shown in Figures 1b and 1c, where the average α phase size of 20% porous sample was found to be 9.3 ± 4.5 μm and that of 10% porosity sample was 13.4 ± 5.5 μm. Similar correlation between the microstructural feature size and fracture morphology of torsional wrought Ti6Al4V alloy [11] and tensile electron beam rapid manufactured Ti6Al4V alloy [17] have been reported. These observations corroborate well known dependence of fracture behavior/morphology on microstructural features/characteristics of Ti alloy samples. The variation in the microstructural features of LENS™ processed porous Ti6Al4V alloy is attributed to the local variations in cooling rates as a consequence of changes in the extent of melting and porosity. It has been reported that the average grain size increases with increasing porosity in laser processed alloy samples [9]. Similar to earlier observations, relatively low α phase size of 10% porous samples than 20% porous samples, apart from porosity, might have also contributed to the better torsional properties of the former samples in the present work.

Figure 3d shows considerable necking of particle-particle contact regions (indicated with circles) in the porous Ti6Al4V alloy samples with 20% porosity. The extensive elongation and necking at the particle-particle bond region suggests that the bonding is very strong in the laser processed alloy, in which the porosity forms as a result of localized melting and subsequent solidification. It is believed that this strong particle to particle bonding in the present laser processed porous Ti6Al4V alloy samples contributed to their ductile and strain hardening behavior comparable to that of fully dense samples.

3.3 Biocompatibility

The *in vitro* MTT assay was used to evaluate the cytotoxicity of laser processed Ti6Al4V alloy samples. In this study, laser processed fully dense samples was used as control because the laser processed Ti6Al4V alloy has been shown to be biocompatible and non-toxic [5]. Figure 4 shows a comparison of cell densities on different Ti alloy samples after 3, 7 and 11 days of culture. Cell proliferation was evident over the duration of experiment and the cell numbers increased with increasing culture time for all samples. Among the samples, dense samples always showed the lowest cell density for all culture duration. Ti6Al4V alloy samples with 10 and 20% showed no statistical difference ($p > 0.05$) in cell density up to day 7. However, at day 11 samples the statistical analysis revealed that the cell density was significantly high ($p < 0.05$) on 20% porosity samples than on 10% porosity samples. These results clearly show that cell proliferation depend on sample porosity. After 3 days of culture, cells proliferated most rapidly on the samples with the highest porosity (20%), in comparison to the 10% porous samples, while the dense samples exhibited lowest cell density. It is believed that the higher surface area and rough surface topography of the pores favors better cellular attachment, which enhances cell proliferation and coverage inside pore areas. The present *in vitro* MTT results demonstrate that these laser processed Ti6Al4V alloy samples are biocompatible and non-toxic.

Although present quasi-static torsional tests on laser processed Ti6Al4V alloy samples show that the presence of porosity can decrease the torsional properties, the inherent brittleness associated solid-state sintered porous materials can be completely eliminated via laser processing. Present results show that matching/close torsional/compressive modulus of biocompatible Ti6Al4V alloy with 20% porosity, with that of human cortical bone, can eliminate stress shielding and significantly improve *in vivo* life of the implants.

NIH-PA Author Manuscript

NIH-PA Author Manuscript

NIH-PA Author Manuscript

4. Conclusions

Laser processed Ti6Al4V alloy samples with total porosities between 0% and 20% were tested for their torsional deformation behavior, mechanical properties and *in vitro* cytotoxicity. The results showed that the samples are biocompatible and porous samples exhibit up to 50% drop in torsional properties. However, microstructural features/characteristics found to have some influence on torsion deformation behavior of porous Ti alloy samples. Laser processed porous Ti6Al4V alloy samples exhibited strain hardening and failed in ductile manner similar to that of fully dense samples. These results suggest that laser processing can eliminate the brittleness associated with porous metals that are produced via conventional powder metallurgical routes.

Acknowledgments

The authors acknowledge the financial support from National Science Foundation (CMMI 0728348) and the Office of Naval Research (N00014-05-0583). Also, the financial support from the W. M. Keck Foundation to purchase a LENS™-750 system at Washington State University is acknowledged.

References

1. Spector, M. Biocompatibility of orthopaedic implants. Williams, DF., editor. CRC Press; Boca Raton, FL: 1982. p. 89-128.
2. Galante J, Rostoker W, Lueck R, Ray RD. J Bone Joint Surg [Am]. 1971; 53A:101.
3. Krishna BV, Bose S, Bandyopadhyay A. Acta Biomater. 2007; 3:997. [PubMed: 17532277]
4. Xue W, Krishna BV, Bandyopadhyay A, Bose S. Acta Biomater. 2007; 3:1007. [PubMed: 17627910]
5. Bandyopadhyay A, España FA, Balla VK, Bose S, Ohgami Y, Davies NM. Acta Biomater. 2010; 6:1640. [PubMed: 19913643]
6. Ryan G, Pandit A, Apatsidis DP. Biomaterials. 2006; 27:2651. [PubMed: 16423390]
7. Krishna BV, Xue W, Bose S, Bandyopadhyay A. JOM. 2008; 60(5):45.
8. Bandyopadhyay A, Krishna BV, Xue W, Bose S. J Mater Sci – Mater Med. 2009; 20:S29. [PubMed: 18521725]
9. Krishna BV, Bose S, Bandyopadhyay A. J Biomed Mater Res Part B – Appl Biomater. 2009; 89B: 481. [PubMed: 18937263]
10. Lee D, Lee YH, Lee S, Lee CS, Hur S. Met Mater Trans A. 2004; 35A:3103.
11. Lee D, Lee S, Lee CS. Mater Sci Eng A. 2004; 366:25.
12. da Silva MG, Ramesh KT. Mater Sci Eng A. 1997; 232:11.
13. Asaoka K, Kuwayama N, Okuno O, Miura I. J Biomed Mater Res. 1985; 19:699. [PubMed: 4077891]
14. Yue S, Pilliar R, Weatherly G. J Biomed Mater Res. 1984; 18:1043. [PubMed: 6544792]
15. Oh IH, Nomura N, Masahashi N, Hanada S. Scripta Mater. 2003; 49:1197.
16. Winn SR, Randolph G, Uludag H, Wong SC, Hair GA, Hollinger JO. J Bone Miner Res. 1999; 14:1721. [PubMed: 10491220]
17. Murr LE, et al. Materials Characterization. 2009; 60:96.
18. Jepsen KJ, Davy DT. J Biomechanics. 1997; 30:891.
19. Dodd B, Atkins AG. Acta Metall. 1983; 34:9.
20. Fleck NA, Hutchinson JW, Tvergaard V. J Mech Phys Solids. 1989; 37:515.

NIH-PA Author Manuscript

NIH-PA Author Manuscript

NIH-PA Author Manuscript

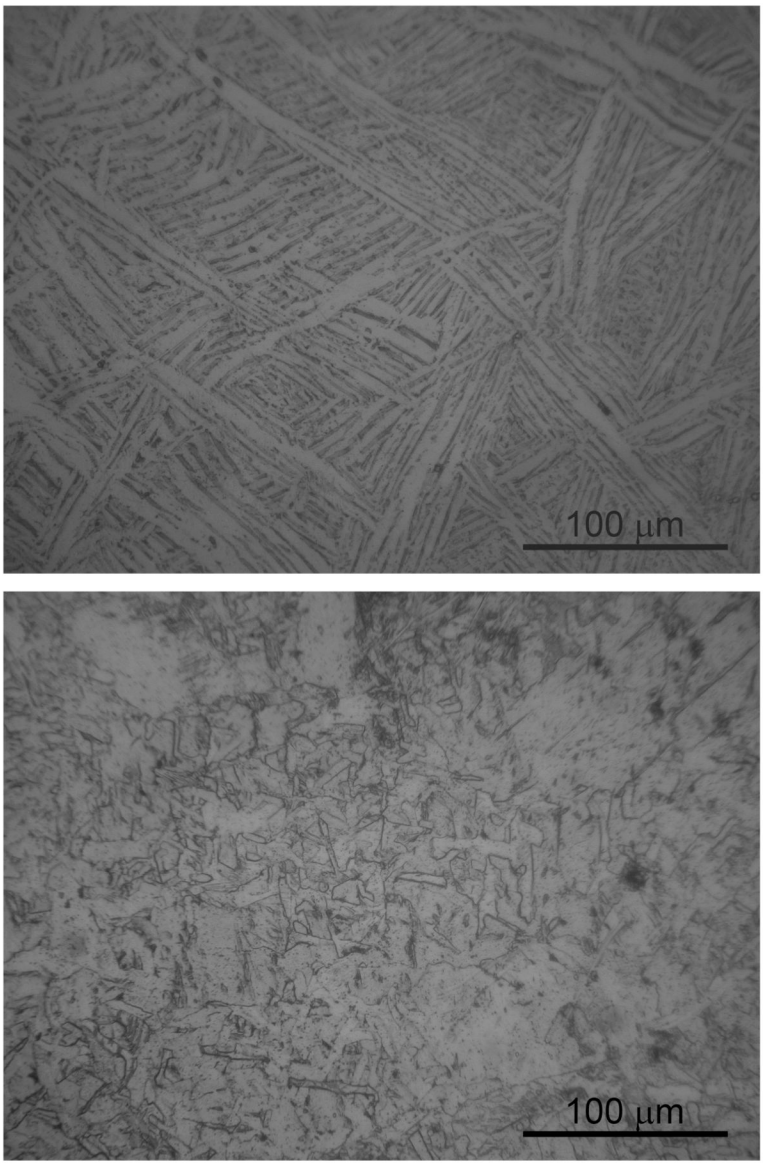

NIH-PA Author Manuscript

NIH-PA Author Manuscript

NIH-PA Author Manuscript

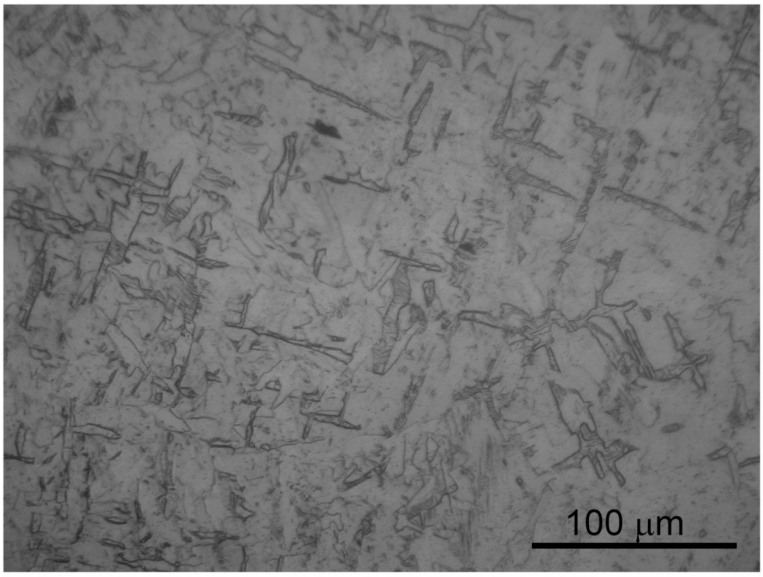

Figure 1.
Microstructures of laser processed Ti6Al4V alloy samples (a) fully dense sample showing typical Widmanstätten microstructure, (b) sample with 10% porosity, (c) sample with 20% porosity.

NIH-PA Author Manuscript

NIH-PA Author Manuscript

NIH-PA Author Manuscript

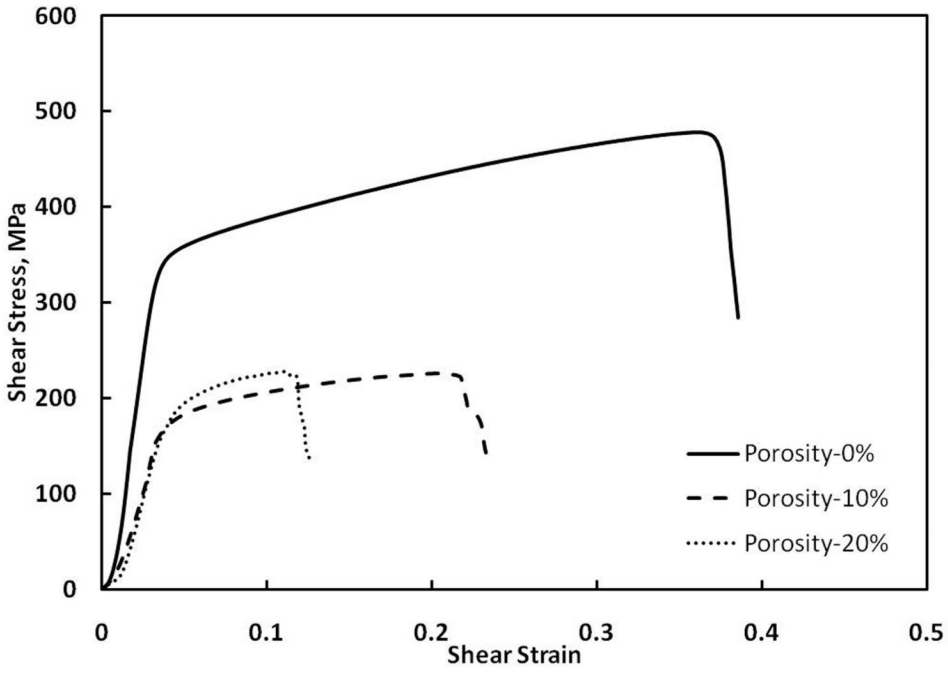

Figure 2.
Typical shear stress – shear strain curves obtained from quasi-static torsional test.

NIH-PA Author Manuscript

NIH-PA Author Manuscript

NIH-PA Author Manuscript

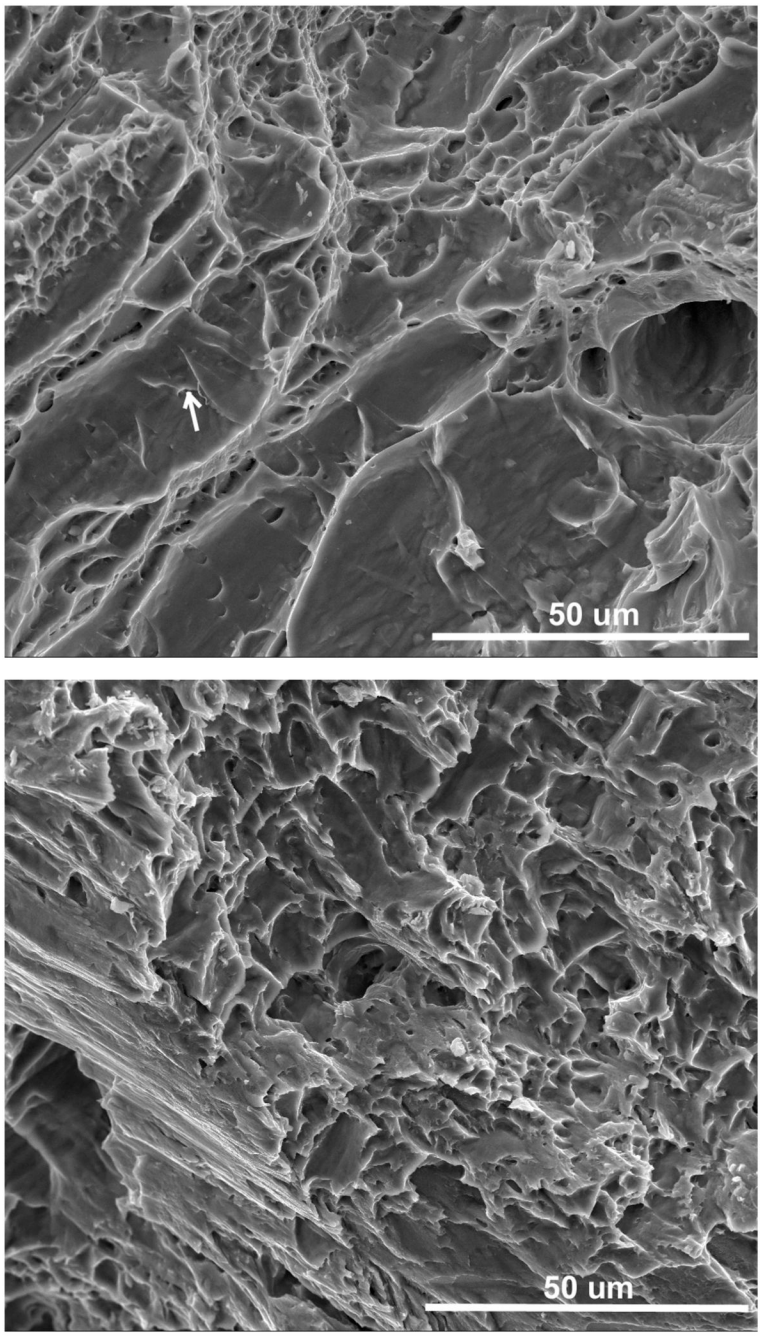

NIH-PA Author Manuscript

NIH-PA Author Manuscript

NIH-PA Author Manuscript

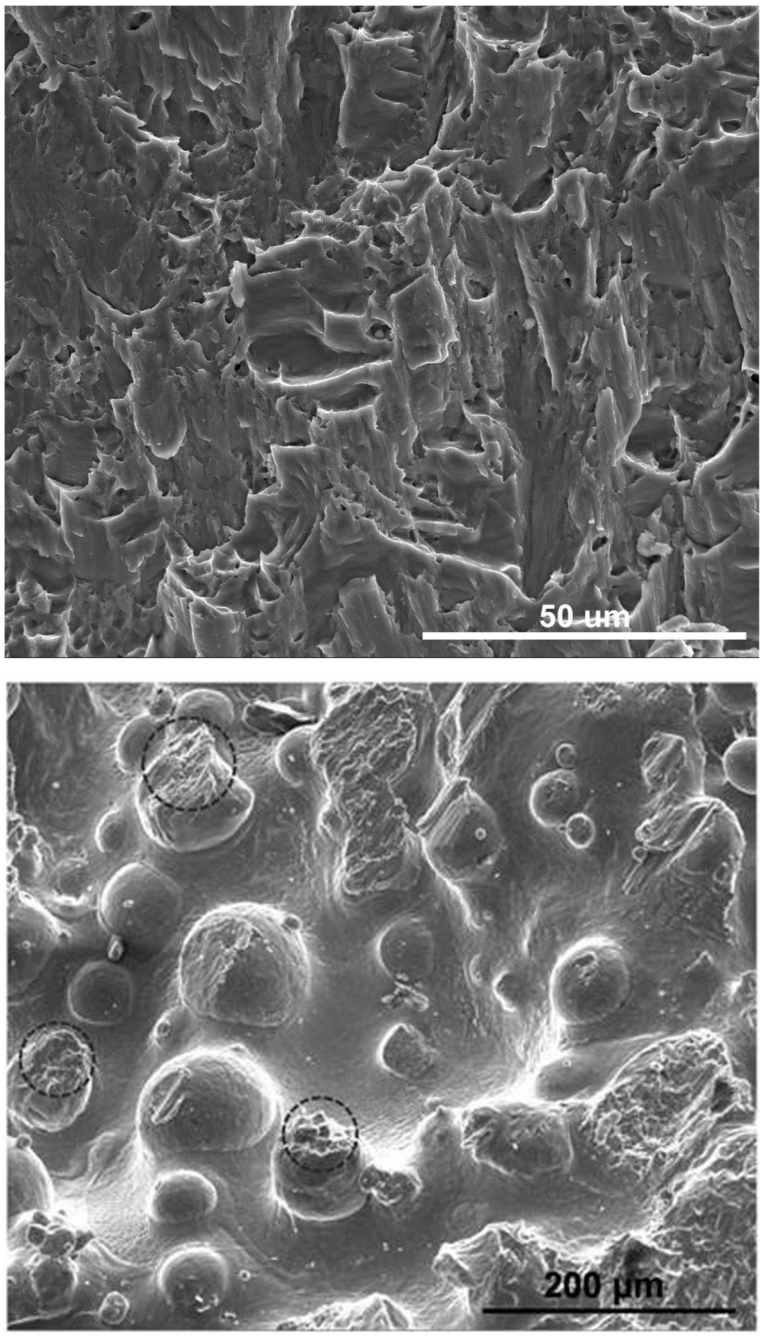

Figure 3.
SEM fractographs of the quasi-statically fractured torsional specimens (a) fully dense sample, (b) sample with 10% porosity, (c) sample with 20% porosity (d) fracture morphology of particle contact regions in the sample with 20 % porosity.

NIH-PA Author Manuscript

NIH-PA Author Manuscript

NIH-PA Author Manuscript

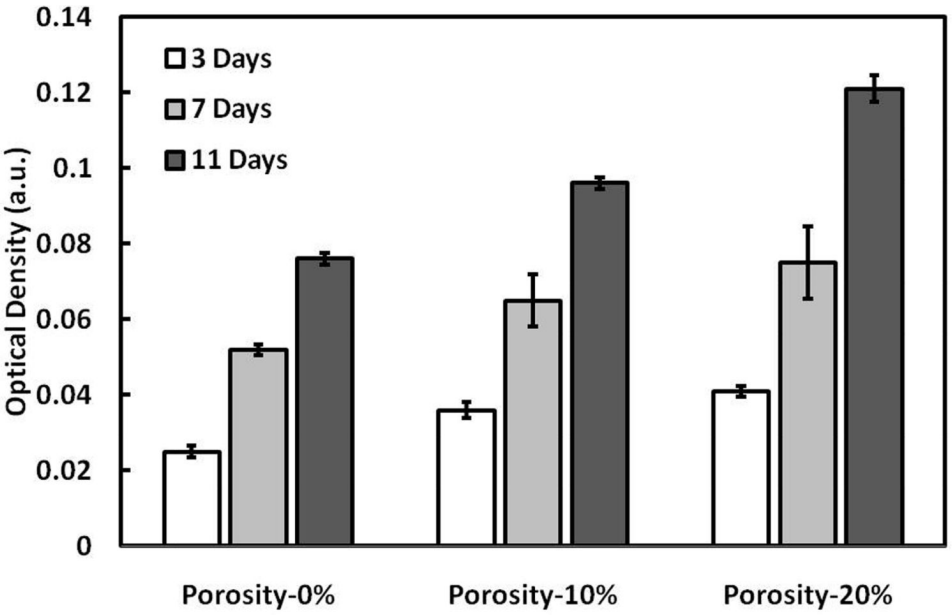

Figure 4.
MTT assay of OPC1 cells on laser processed Ti6Al4V alloy samples. Higher optical density represents higher concentration of living cells.

NIH-PA Author Manuscript NIH-PA Author Manuscript NIH-PA Author Manuscript

Table 1

Quasi-static compression and torsional properties of laser processed porous Ti6Al4V alloy samples. For comparison torsional properties of human cortical bone are also included [18].

	Average Compression Properties				
Porosity (%)	**Young's Modulus (GPa)**			**0.2% Proof Strength (MPa)**	
0 ± 0.8	104 ± 2			1014 ± 20	
10 ± 1.3	79 ± 7			932 ± 10	
20 ± 1.8	46 ± 8			764 ± 17	
p value	0.02			0.02	
	Average Torsional Properties				
	Yield Strength (MPa)	**Modulus (GPa)**	**Max. Shear Stress (MPa)**	**Shear Strain @ max. Shear Stress**	**Max. Shear Strain**
0 ± 0.5	332 ± 22	11 ± 1.3	455 ± 31	0.37 ± 0.001	0.40 ± 0.01
10 ± 2.0	190 ± 2	10 ± 0.2	235 ± 13	0.26 ± 0.06	0.29 ± 0.06
20 ± 1.5	185 ± 1	5.7 ± 0.4	233 ± 7	0.11 ± 0.07	0.12 ± 0.02
Human Cortical Bone [18]	55.8 ± 3.8	5.0 ± 0.2	74.1 ± 3.2	0.052 ± 0.009	0.052 ± 0.009
p value	0.07	0.52	0.006	0.006	0.007